Inorganic Chemistry

Article

pubs.acs.org/IC

$\{Sn_9[Si(SiMe_3)_3]_3\}^-$ and $\{Sn_8Si[Si(SiMe_3)_3]_3\}^-$: Variations of the E_9 Cage of Metalloid Group 14 Clusters

Claudio Schrenk,[†] Marco Neumaier,[‡] and Andreas Schnepf*[,†]

[†]Institute of Inorganic Chemistry, University of Duisburg-Essen, Universitätsstrasse 5-7, D-45117 Essen, Germany

[‡]Institute of Inorganic Chemistry, Karlsruhe Institute of Technology (KIT), KIT-Campus Süd, Postfach 6980, D-76049 Karlsruhe, Germany

Supporting Information

ABSTRACT: The disproportionation reaction of the subvalent metastable halide SnBr proved to be a powerful synthetic method for the synthesis of metalloid cluster compounds of tin. Hence, the neutral metalloid cluster compound $Sn_{10}[Si(SiMe_3)_3]_6$ (**3**) was synthesized from the reaction of SnBr with $LiSi(SiMe_3)_3$. In the course of the reaction anionic clusters might also be present, and we now present the first anionic cluster compound $\{Sn_8E[Si(SiMe_3)_3]_3\}^-$ (E = Si, Sn), where one position in the cluster core is occupied by a silicon or a tin atom, giving further insight into structural variations of E_9 cages in metalloid group 14 cluster compounds.

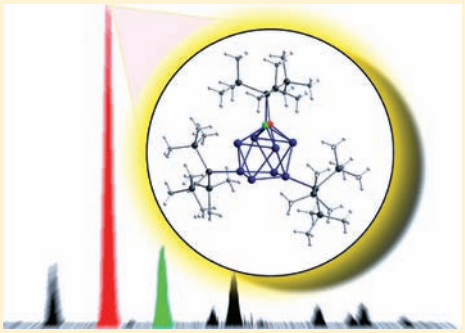

INTRODUCTION

Metalloid clusters of tin of the general formulas Sn_nR_m ($n > m$; R = ligand like $Si(SiMe_3)_3$ or $NSiMe_3Dipp$; Dipp = 2,6-iPr_2-C_6H_3) might be seen as model compounds for the area between the molecular and solid state, as the average oxidation state of the tin atoms is between 1 and 0, approaching the value 0 of the bulk phase on increasing the number of tin atoms (n) with respect to the number of ligands (m). For the synthesis of such molecular metalloid compounds the main synthetic routes applied[1] are the reductive Wurtz-type coupling reaction of a halide or the disproportionation reaction of a subvalent metastable halide like Sn^IBr.[2] Thereby in recent years metalloid cluster compounds with up to 17 tin atoms in the cluster core could be synthesized, where different structural motives are present. Thus, the arrangement of the 17 tin atoms in the metalloid cluster $Sn_{17}\{GaCl(ddp)\}_4$ (**1**; ddp = HC-$(CMeNC_6H_3$-2,6-$iPr_2)_2$) can be described as two Sn_9 units linked by a central tin atom.[3] In addition to this the arrangement of the tin atoms inside the Sn_{15} cluster $Sn_{15}[(NSiMe_3)Dipp]_6$ (**2**; Dipp = 2,6-iPr_2-C_6H_3)[4] can be described as a section of a *bcc* structure, realized for elemental tin only at a pressure of around 45 ± 5 GPa.[5] Additionally, the tin atoms in the Sn_{10} cluster $Sn_{10}[Si(SiMe_3)_3]_6$ (**3**) build up a centaur polyhedron,[6] i.e. a polyhedron that can be described as a fusion of different polyhedra; in the case of **3** this is a cube and an icosahedron. Consequently a great structural diversity is present in the field of metalloid cluster compounds of tin, and to date no concrete route allocated by larger clusters on the way to the elemental state is identified. However, in the case of the Sn_{17} cluster **1** the outstanding stability of the Sn_9 unit becomes obvious, which was also identified recently by calculations for larger clusters with up to 20 tin atoms.[7] Additionally, gas-phase measurements of large anionic and cationic clusters show that larger clusters are best described as a fusion of small clusters where the Sn_9 unit is also of central relevance.[8] The special role of the E_9 unit is also obvious from the area of Zintl anions, where Sn_9^{x-} (x = 2−4) anions are the most prominent starting material.[9]

The first metalloid Sn_9 cluster compound, Sn_9Ar_3 (**4**; Ar = 2,6-$trip_2$-C_6H_3; trip = 2,4,6-iPr_3-C_6H_2), was synthesized by Power et al. via the thermolysis of SnArH in hot toluene.[10] The Sn_9 framework of **4** can be described as a tricapped-trigonal-prismatic closo structure with a large height (412 pm) to edge (300 pm) ratio of the prism of 1.37. However, the open-shell structure seems unusual, and it is questionable if a comparable anionic or cationic closed-shell diamagnetic compound can be obtained. In the following we now describe the synthesis and structure of such an anionic compound.

RESULTS AND DISCUSSION

In the case of germanium the anionic Ge_9 cluster compound $\{Ge_9[Si(SiMe_3)_3]_3\}^-$ (**5**) is obtained in ca. 30% yield by the reaction of the monohalide GeBr with $LiSi(SiMe_3)_3$[11] or by the reaction of the Zintl anion Ge_9^{4-} with $ClSi(SiMe_3)_3$ in ca. 80% yield.[12] As the Ge_9 core in **5** is shielded rather incompletely by the three $Si(SiMe_3)_3$ ligands, **5** is highly reactive and can be used for further build-up reactions leading to $Ge_{18}M[Si(SiMe_3)_3]_6^n$ clusters (n = −1, M = Cu, Ag, Au; n = 0, M = Zn, Cd, Hg).[13] Due to the incomplete shielding **5** can also be used as a ligand in coordination chemistry, where a cluster enlargement takes place.[14]

Received: August 9, 2011
Published: March 21, 2012

   dx.doi.org/10.1021/ic201730g | *Inorg. Chem.* 2012, 51, 3989−3995

In the case of tin, a comparable reaction of a metastable $Sn^{I}Br$ solution with $LiSi(SiMe_3)_3$ first of all leads to the neutral metalloid cluster $Sn_{10}[Si(SiMe_3)_3]_6$ (**3**) in 17% yield.[6] However, storing the reaction solution at −28 °C leads first of all to the formation of a black oil, which can be separated. Dissolving this oil in Et_2O yields a black solution. Mass spectroscopic investigations of this black solution, applying the mild electrospray ionization (ESI)[15] technique, show that a couple of anionic clusters are present inside this solution (Figure 1).

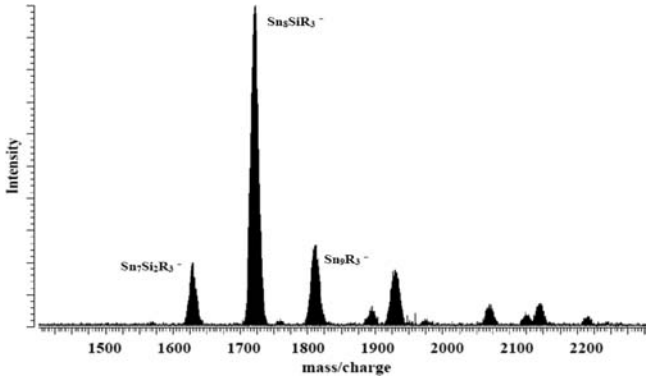

Figure 1. Mass spectrum of the black ether solution from the reaction of SnBr with $LiSi(SiMe_3)_3$ applying electrospray ionization.

The signal with the greatest intensity can be clearly assigned to the anionic cluster of the composition $\{Sn_8Si[Si(SiMe_3)_3]_3\}^-$ ($\mathbf{6_{Si}}$; m/z 1728.55) by a comparison of the calculated and measured isotopic patterns (Figure 2). Additionally, less intense signals of $\{Sn_9[Si(SiMe_3)_3]_3\}^-$ ($\mathbf{6_{Sn}}$; m/z 1820.47) and $\{Sn_7Si_2[Si(SiMe_3)_3]_3\}^-$ ($\mathbf{6_{Si2}}$; m/z 1636.62) are observed together with signals of anionic clusters with higher masses which cannot be identified directly by their isotopic pattern due to a small intensity, leading to a bad signal-to-noise ratio.

Nevertheless, this result shows that in addition to the neutral cluster $Sn_{10}[Si(SiMe_3)_3]_6$ (**3**) also anionic clusters are formed by the reaction of a metastable $Sn^{I}Br$ solution with $LiSi(SiMe_3)_3$, and on concentrating the ether solution we finally were able to obtain another product of the reaction in the form of dark red, nearly black crystals. X-ray crystal structure analysis of these crystals reveals that the anionic $\{E_9[Si(SiMe_3)_3]_3\}^-$ cluster **6** is present, crystallizing together with $[Li(Et_2O)_2(THF)_2]^+$ as the countercation.

The molecular structure of **6** is shown in Figure 3 and is best described as a monocapped-square-antiprismatic arrangement of nine heavy atoms where the capping atom (Sn3/Si3a) and two of the base square atoms (Sn1 and Sn2) are bound to a ligand.

However, during refinement of the crystal structure it became obvious that the capping atom (Sn3/Si3a) must be heavier than a silicon atom and lighter than a tin atom. As tin and silicon are the only atoms heavier than oxygen that fit within this position and which were used during the reaction course, this finding can only be explained assuming that two different molecules crystallize together, which only differ in that special atom position. Applying this model, the crystal structure could be refined, leading to an occupation at this position of 74% and 26% of Si and Sn, respectively. Hence, inside the crystal the anion $\{Sn_9[Si(SiMe_3)_3]_3\}^-$ ($\mathbf{6_{Sn}}$) crystallizes together with anionic $\{Sn_8Si[Si(SiMe_3)_3]_3\}^-$ ($\mathbf{6_{Si}}$), where the ligand-bound tin atom (Sn3) is substituted by a silicon atom (Si3a). The silicon atom (Si3a) must thereby come from the degradation of a $Si(SiMe_3)_3$ ligand, which seems plausible, as also $Si(SiMe_3)_4$ is obtained during the reaction in substantial amounts, as identified by ^{29}Si NMR spectroscopy (signal at −134 ppm[16] for the central silicon atom). A similar degradation of the $Si(SiMe_3)_3$ ligand was recently observed during the synthesis of $\{(SiMe_3)_2SiGa_4[Si(SiMe_3)_3]_3\}^-$,[17] $\{(SiMe_3)_2SiAl_4[Si(SiMe_3)_3]_3\}^-$,[18] $Sn_4Si(Si(SiMe_3)_3)_4(SiMe_3)_2$,[19] and $\{Ge_{10}Si[Si(SiMe_3)_3]_4(SiMe_3)_2Me\}^-$.[20] Additionally, such a dismantling of the $Si(SiMe_3)_3$ ligand was recently observed in the gas phase via collision-induced dissociation experiments starting from $\{Ge_9[Si(SiMe_3)_3]_3\}^-$ (**5**), leading at the end to $[Ge_9Si]^-$, where also one silicon atom of a $Si(SiMe_3)_3$ ligand is incorporated, leading to a cluster enlargement.[21] The occupation of $\mathbf{6_{Si}}$ and $\mathbf{6_{Sn}}$ of 74% to 26% inside the crystal lattice nearly fits the intensity in the mass spectra, where the signal height for $\mathbf{6_{Sn}}$ is only ca. 30% of that of $\mathbf{6_{Si}}$ (Figure 1): i.e., the intensity

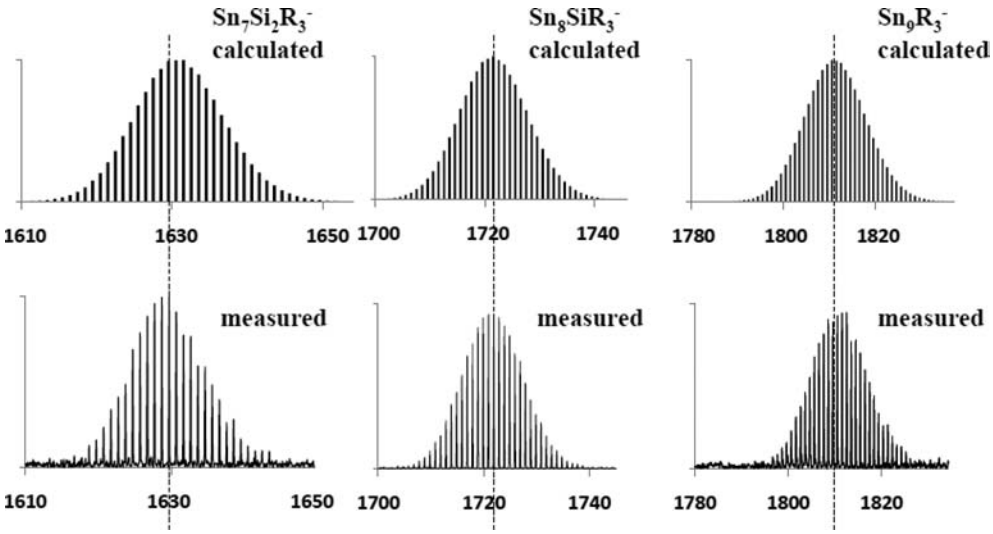

Figure 2. Calculated and measured isotopic patterns of (right) $\{Sn_9[Si(SiMe_3)_3]_3\}^-$ ($\mathbf{6_{Sn}}$), (middle) $\{Sn_8Si[Si(SiMe_3)_3]_3\}^-$ ($\mathbf{6_{Si}}$), and (left) $\{Sn_7Si_2[Si(SiMe_3)_3]_3\}^-$ ($\mathbf{6_{Si2}}$).

dx.doi.org/10.1021/ic201730g | Inorg. Chem. 2012, 51, 3989−3995

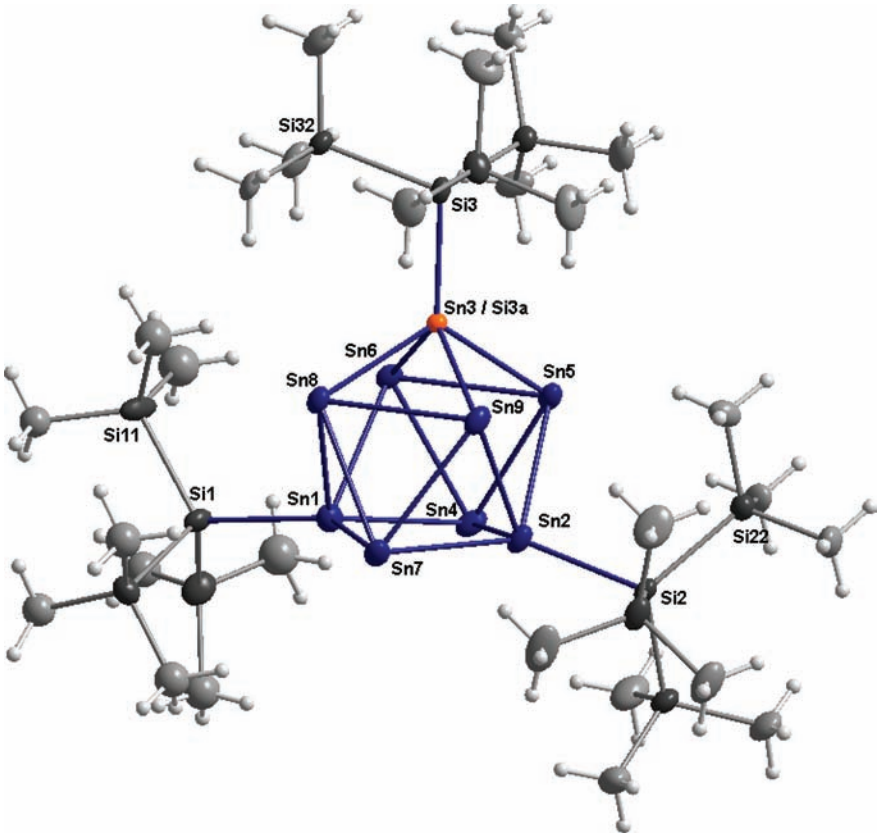

Figure 3. Molecular structure of $\{Sn_9[Si(SiMe_3)_3]_3\}^-/\{Sn_8Si[Si(SiMe_3)_3]_3\}^-$ ($\mathbf{6}_{Sn}/\mathbf{6}_{Si}$). Thermal ellipsoids are shown at the 25% probability level. For the split position Sn3/Si3a and Si3/Si3b only the tin atom and Si3 are shown. Selected bond distances (pm) and angles (deg): Sn(1)−Sn(4) = 289.35(12), Sn(1)−Sn(7) = 291.08(12), Sn(1)−Sn(8) = 295.43(12), Sn(3)−Sn(8) = 266(2), Sn(3)−Sn(6) = 269.3(19), Sn(3)−Sn(9) = 271.7(19), Sn(3)−Sn(5) = 273.4(16), Si(3A)−Si(3B) = 228(4), Si(3A)−Sn(5) = 262(3), Si(3A)−Sn(9) = 269(3), Si(3A)−Sn(6) = 289(3), Si(3A)−Sn(8) = 295(3), Sn(5)−Sn(6) = 313.12(13), Sn(5)−Sn(9) = 348.6(1), Sn(8)−Sn(9) = 313.34(13), Sn(6)−Sn(8) = 338.9(1), Sn(2)−Si(2) = 258.5(3), Sn(3)−Si(3) = 251(6), Si(2)−Si(22) = 234.9(4); Sn(4)−Sn(1)−Sn(7) = 99.79(4), Sn(8)−Sn(1)−Sn(6) = 69.86(3), Sn(8)−Sn(3)−Sn(5) = 118.6(6), Sn(6)−Sn(3)−Sn(5) = 70.5(4), Sn(5)−Si(3A)−Sn(8) = 112.9(9), Sn(6)−Si(3A)−Sn(8) = 70.9(6), Sn(1)−Sn(4)−Sn(2) = 80.02(3), Sn(3)−Sn(5)−Sn(2) = 94.1(4).

distribution in the mass spectrum seems to resemble the proportions of the anionic clusters in solution.[22]

This interpretation shows that $\mathbf{6}_{Si}$ can be substituted by $\mathbf{6}_{Sn}$ inside the crystal lattice and vice versa, which is only possible if both compounds exhibit a similar arrangement. Hence, to verify that such a substitution is possible, we calculated the gas-phase structure of $\mathbf{6}_{Sn}$ and $\mathbf{6}_{Si}$ via quantum chemical calculations.[23] The calculations thereby show that the substitution of the tin atom by a silicon atom only leads to minor changes in the arrangement of the remaining eight tin atoms and the three $Si(SiMe_3)_3$ ligands. Hence, the Sn−Sn distances inside $\mathbf{6}_{Sn}$ (E = Sn) and $\mathbf{6}_{Si}$ (E = Si) only differ by ca. 5 pm, while the Sn−E distance to the capping E atom differs by 24 pm.[24] This result clearly indicates that $\mathbf{6}_{Sn}$ and $\mathbf{6}_{Si}$ can indeed cocrystallize in one crystal lattice, statistically occupying the anion position. During the calculations we also found that the capping tin atom in $\mathbf{6}_{Sn}$ has a slightly immersed position, as the calculated Sn−Si distance is at 261 pm shorter than the remaining two Sn−Si bonds (264 pm): i.e., the position for the substitution is already obvious inside the Sn_9 compound. Additionally the reaction $\mathbf{6}_{Sn}$ + Si → $\mathbf{6}_{Si}$ + Sn is exothermic by 137 kJ/mol. However, $\mathbf{6}_{Si}$ will not form by the substitution of a Sn atom in $\mathbf{6}_{Sn}$ by a silicon atom. It might be rather expected that $\mathbf{6}_{Si}$ will form from a Sn_8R_x precursor molecule ($x > 3$) where one $Si(SiMe_3)_3$ ligand is dismantled, leading to the naked Si atom, which is then incorporated into the cluster core (vide supra[16−20]).

Nevertheless, due to the statistic occupation in the cocrystal $\mathbf{6}_{Si}/\mathbf{6}_{Sn}$ the experimental Sn−Sn and Sn−Si distances show large standard deviations, as not all heavy-atom positions could be refined for the separated molecules. Hence, we tried to obtain $\mathbf{6}_{Si}$ or $\mathbf{6}_{Sn}$ or both together in another crystal system where no statistic occupation is present by changing the complexing reagent of the lithium cation. Thereby, the addition of the crown ether 12-crown-4 leads to the formation of black crystals showing a different crystal system. The crystal structure solution of these crystals reveals that $\mathbf{6}_{Sn}$ now crystallizes alone with the cation $\{Li(12\text{-crown-}4)_2\}^+$. The molecular structure of $\mathbf{6}_{Sn}$ is given in Figure 4, showing slight differences from the structure found in the cocrystal $\mathbf{6}_{Si}/\mathbf{6}_{Sn}$.

This time the nine tin atoms are arranged in the form of a tricapped trigonal prism, where the Sn−Sn distances between naked tin atoms are, at 305.6 pm, slightly longer than the Sn−Sn distance between the naked and ligand-bound tin atoms, where an average tin−tin distance of 288.9 pm is found. This result clearly indicates that the arrangement of the nine tin atoms within $\mathbf{6}_{Sn}$ is quite flexible with respect to the requirement of the surroundings: e.g., crystal packing. The height (387.4 pm) to edge (305.6 pm) ratio of the prism is 1.27, thus being a bit smaller than that found within the neutral

dx.doi.org/10.1021/ic201730g | Inorg. Chem. 2012, 51, 3989−3995

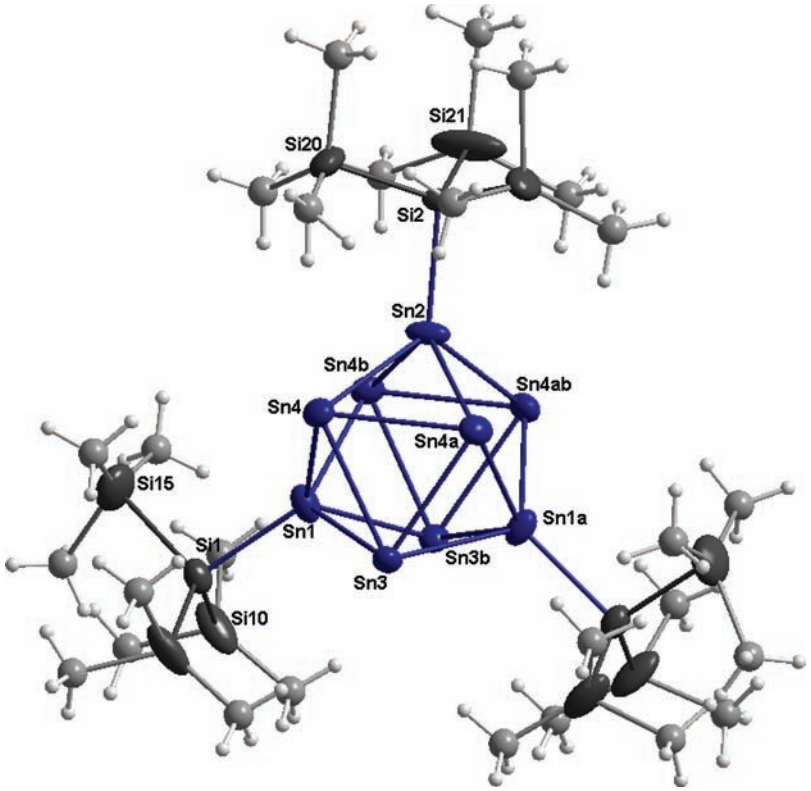

Figure 4. Molecular structure of $\{Sn_9[Si(SiMe_3)_3]_3\}^-$ ($\mathbf{6_{Sn}}$). Thermal ellipsoids are shown for Sn and Si at the 25% probability level. Selected bond distances (pm) and angles (deg): Sn(1)−Sn(3) = 288.56(10), Sn(1)−Sn(4) = 286.84(11), Sn(2)−Sn(4) = 289.16(9), Sn(3)−Sn(4) = 305.74(10), Sn(4)−Sn(4a) = 305.47(15), Sn(3)−Sn(3b) = 376.1(1), Sn(4)−Sn(4b) = 393.4(1), Sn(1)−Si(1) = 252.7(4), Sn(2)−Si(2) = 254.2(4), Si(1)−Si(10) = 228.4(6), Si1−Si15 = 240.1(9), Si(2)−Si(20) = 238.5(7), Si2−Si21 = 227.6(9); Sn(4)−Sn(1)−Sn(4b) = 86.58(4), Sn(4)−Sn(3)−Sn(4a) = 59.94(3), Sn(4)−Sn(1)−Sn(3) = 64.19(3).

Table 1. Values of α^a for Calculated Anionic $Sn_9R_3^-$ (Second Column) and Neutral Sn_9R_3 (Third Column) Clusters

R	α [°] $Sn_9R_3^{1-}$	α [°] Sn_9R_3
H	20.0	12.9
Me	17.5	15.7
Ph	18.5	11.9
SiH_3	23.9	23.7
$Si(SiMe_3)_3$ $\mathbf{6_{Sn}}$·$\mathbf{6_{Si}}$	22.4	
(measured) $\mathbf{6_{Sn}}$	3.8	
2,6-trip$_2$-C_6H_3; trip = 2,4,6-*i*Pr$_3$-C_6H_2 (measured)[10]		2.2

[a]Graphical clarification is given by the schematic presentation on the right.

compound Sn_9Ar_3 **4** but exactly the same as that found for the isostructural Ge_9 compound **5**.

Structure and Electronics. Both clusters discussed here ($\mathbf{6_{Sn}}$ and $\mathbf{6_{Si}}$) exhibit 22 bonding electrons, and due to Wade's rules[25] a nido cluster might be expected and is found on first glance for the cocrystal $\mathbf{6_{Sn}}$/$\mathbf{6_{Si}}$, where a slightly distorted E_9 cluster core of a monocapped square antiprism is present; i.e., the Sn−Sn distances in the capped Sn_4 rectangle (Sn5, Sn6, Sn8, Sn9) are quite different (313 and 344 pm). Despite this, when $\mathbf{6_{Sn}}$ crystallizes together with the cation Li(12-crown-4)$_2$}$^+$ a closo structure of a tricapped-trigonal-prismatic arrangement (D_{3h}) is realized, as was also found in the case of the neutral cluster Sn_9Ar_3 **4** (Ar = 2,6-trip$_2$-C_6H_3; trip = 2,4,6-*i*Pr$_3$-C_6H_2), which possesses 21 bonding electrons, indicating that the E_9 core is easily modified depending on external influences, such as the number of electrons, ligand, and crystal-packing forces. To further elucidate the influence of the ligand and the number of electrons inside the cluster core, we performed quantum chemical calculations on neutral and anionic $Sn_9R_3^x$ clusters (R = H, CH_3, Ph, SiH_3; x = 0, −1).

dx.doi.org/10.1021/ic201730g | Inorg. Chem. 2012, 51, 3989−3995

Thereby the change of the structure of the cluster core is best illustrated by comparing the angle α between the triangular faces defined by three naked tin atoms (Table 1).

As can be seen from Table 1, the changes in α are small on changing the ligand, indicating that there is only a minor electronic influence by the ligand.[26] Additionally the calculations show that also in the case of the neutral compound the distorted-monocapped-square-antiprismatic structure (C_{2v}) is more stable than the D_{3h} structure. However, the energetic difference between the distorted ($\alpha > 0°$) and the undistorted tricapped-trigonal-prismatic structures ($\alpha = 0°$) is small (less than 10 kJ/mol for the anionic as well as for the neutral model compound[27]), leading to a highly flexible system within the cluster core with different possible arrangements depending on the external requirements.

Nevertheless a major difference between the neutral compound **4** and $\mathbf{6_{Sn}}$ is the fact that the Sn_9 core is completely shielded by the three ligands in the case of **4**, while it is quite open in the case of $\mathbf{6_{Sn}}$, where the ligands incompletely shield the cluster core (Figure 5). This opens the possibility for

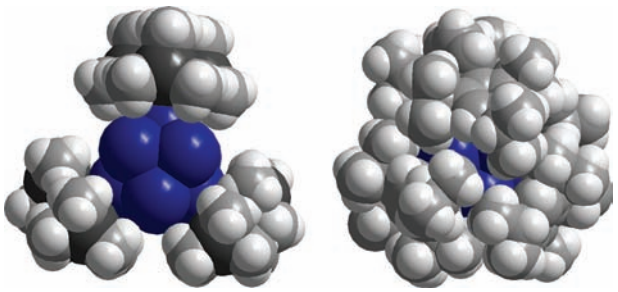

Figure 5. Space-filling models of (left) $\{Sn_9[Si(SiMe_3)_3]_3\}^-$ ($\mathbf{6_{Sn}}$) and (right) Sn_9Ar_3 (**4**; Ar = 2,6-trip$_2$-C_6H_3; trip = 2,4,6-*i*Pr$_3$-C_6H_2): view toward the three naked tin atoms.

further reactions, as was recently shown for the isostructural germanium compound $\{Ge_9[Si(SiMe_3)_3]_3\}^-$ (**5**), which also exhibits the structure of a tricapped trigonal prism with an height to edge value of the prism of 1.27, identical with that found for $\mathbf{6_{Sn}}$.

SUMMARY AND OUTLOOK

In summary, we have presented the synthesis and structure of the first monoanionic metalloid Sn_9 cluster, $\{Sn_9[Si(SiMe_3)_3]_3\}^-$ ($\mathbf{6_{Sn}}$), which cocrystallizes together with the structurally similar cluster $\{Sn_8Si[Si(SiMe_3)_3]_3\}^-$ ($\mathbf{6_{Si}}$), where one ligand-bound tin atom is substituted by a silicon atom, which results from the fragmentation of a $Si(SiMe_3)_3$ ligand. On changing the countercation, a second solid-state structure of $\mathbf{6_{Sn}}$ is obtained. In the different solid-state structures the nine tin atoms within $\mathbf{6_{Sn}}$ are arranged in the form of a distorted tricapped trigonal prism or a distorted monocapped square antiprism. Quantum chemical calculations show that the difference between these two arrangements of the nine tin atoms is small, leading to a flexible Sn_9 core.

The less shielded Sn_9 cluster core of the anionic clusters $\mathbf{6_{Sn}}$/$\mathbf{6_{Si}}$ now opens the possibility for subsequent reactions in the future, perhaps giving access to larger aggregates as has been possible in recent years for the comparable anionic cluster $\{Ge_9[Si(SiMe_3)_3]_3\}^-$ (**5**).[13,14]

EXPERIMENTAL SECTION

All operations were carried out under an atmosphere of dry argon or nitrogen using modified Schlenk line and glovebox techniques. The cocondensation reaction was performed in a homemade cocondensation apparatus.[28] All solvents were freshly distilled from sodium and degassed immediately prior to use. The ^1H and ^{13}C NMR spectroscopic data were recorded on a Bruker AV 400 spectrometer. Mass spectrometric experiments were performed on an IonSpec Ultima FT-ICR-MS (Fourier transform ion cyclotron resonance mass spectrometer), equipped with a 7 T superconducting magnet, coupled to a home-built electrospray ionization source (ESI).

Synthesis of $\{Sn_9[Si(SiMe_3)_3]_3/Sn_8Si[Si(SiMe_3)_3]_3\}[Li(THF)_2(Et_2O)_2]$ ($\mathbf{6_{Sn}/6_{Si}}$). A metastable Sn^IBr solution was prepared applying a cocondensation technique, where elemental tin (2.08 g; 17.6 mmol) reacted with 20 mmol of HBr at 1240 °C and where the resulting Sn^IBr was condensed at −196 °C with a mixture of toluene and NBu_3 in a volume ratio of 4:1. After the temperature was raised to −78 °C, a solution of 10.6 g (22 mmol) of $LiSi(SiMe_3)_3 \cdot 3THF$ in 50 mL of toluene was added. The reaction mixture was slowly warmed to room temperature, and a black reaction solution was obtained. Storing this solution at −28 °C led to a black oil. The solution was decanted, and the oil was washed with pentane, leading to an almost solid black residue. Afterward the residue was dissolved in 10 mL of ether, leading to a nearly black solution. Storing this ether solution at 6 °C for 1 week led to dark red, nearly black rodlike crystals of $\{Sn_9[Si(SiMe_3)_3]_3/Sn_8Si[Si(SiMe_3)_3]_3\}[Li(THF)_2(Et_2O)_2]$ (100 mg, 0,05 mmol, 2.2%). ^1H NMR (THF-d_8): δ 0.19 (s, 54 H, $\mathbf{6_{Sn}/6_{Si}}$ $SnSi(SiMe_3)_3$), 0.23 (s, 27 H (25%), $\mathbf{6_{Sn}}$ $SnSi(SiMe_3)_3$), 0.24 (s, 27 H (75%), $\mathbf{6_{Si}}$ $SiSi(SiMe_3)_3$). $^{13}C\{^1H\}$ NMR (THF-d_8): δ 2.4 (s, $\mathbf{6_{Sn}/6_{Si}}$ $SnSi(SiMe_3)_3$), 3.7 (s, $\mathbf{6_{Sn}/6_{Si}}$ $ESi(SiMe_3)_3$).

The addition of 12-crown-4 to a thf solution of $\mathbf{6_{Sn}}$ led to the formation of black blocklike crystals of $[Sn_9(Si(SiMe_3)_3)_3][Li(12\text{-crown-}4)_2]$.

Mass Spectrometry. The cluster $\{Sn_9[Si(SiMe_3)_3]_3\}^-/\{Sn_8Si[(Si(SiMe_3)_3]_3\}^-$ ($\mathbf{6_{Sn}/6_{Si}}$) was brought into the gas phase by electrospraying a THF solution of $\mathbf{6_{Sn}/6_{Si}}$. The end plate of the electrospray source was typically held at a potential of +3.2 kV relative to the electrospray needle, which was grounded. A potential of +3.3 kV was applied to the entrance of the metal-coated quartz capillary.

X-ray Structural Characterization. Table 2 contains the crystal data and details of the X-ray structural determination for $\{Sn_9[Si(SiMe_3)_3]_3/Sn_8Si[Si(SiMe_3)_3]_3\}[Li(THF)_2(Et_2O)_2]$ ($\mathbf{6_{Si}/6_{Sn}}$) and $[Sn_9[Si(SiMe_3)_3]_3][Li(12\text{-crown-}4)_2]$ ($\mathbf{6_{Sn}}$). The data were collected at 150 K ($\mathbf{6_{Si}/6_{Sn}}$) or 200 K ($\mathbf{6_{Sn}}$) on a STOE IPDS II ($\mathbf{6_{Si}/6_{Sn}}$) or Bruker APEX II ($\mathbf{6_{Sn}}$) diffractometer employing monochromated Mo Kα (λ = 0.710 73 Å) radiation from a sealed tube and equipped with an Oxford Cryosystems cryostat. The structure was solved by direct methods and refined by full-matrix least-squares techniques (programs used: SHELXS and SHELXL[29]). The non-hydrogen atoms were refined anisotropically, and the hydrogen atoms were calculated using a riding model. $\mathbf{6_{Si}/6_{Sn}}$: inside the crystal $Sn_9[Si(SiMe_3)_3]_3^-$ and $Sn_8Si[Si(SiMe_3)_3]_3^-$ occupy the same position in a way that only one ligand bound tin atom is substituted by a silicon atom. This disorder is described during refinement by a split model where the two positions are correlated by a variable which refines to an occupation of 0.74 for silicon and 0.26 for tin. Additionally the directly bound silicon atom of the $Si(SiMe_3)_3$ group is split (Si3, Si3b), refining to the same occupation (0.74 for Si3b and 0.26 for Si3). However, splitting of the atoms of the $SiMe_3$ groups was not possible. Due to the large unit cell many reflections are overlapped and omitted during data collection. Additionally, the reflections are quite broad, which might be due to the poor fit of $Sn_9(Si(SiMe_3)_3)_3^-$ and $Sn_8Si(Si(SiMe_3)_3)_3^-$. During refinement only reflections with a 2θ value lower than 45° were used. $\mathbf{6_{Sn}}$: due to a severe disorder of the $Si(SiMe_3)_3$ ligands, which was described by a split model together with a racemic twinning of the crystal that was described by the twin matrix −1000−1000−1 (BASF value refines to 0.305 91), the crystals only diffract well up to a 2θ value of 50°. Thus, only reflections with a 2θ value lower than 50° were used during refinement. CCDC-837278 ($\mathbf{6_{Si}/6_{Sn}}$) and CCDC-

dx.doi.org/10.1021/ic201730g | Inorg. Chem. 2012, 51, 3989−3995

Table 2. Crystal Data and Details of Structural Determinations

	$\{Sn_9[Si(SiMe_3)_3]_3$/ $Sn_8Si[Si(SiMe_3)_3]_3\}$ $[Li(THF)_2(Et_2O)_2]$ ($\mathbf{6_{Si}}$/$\mathbf{6_{Sn}}$)	$\{Sn_9[Si(SiMe_3)_3]_3\}$ $[Li(12\text{-crown}[4])_2]$ ($\mathbf{6_{Sn}}$)
formula	$Sn_9Si_{12}C_{43}LiO_4H_{117}$/ $Sn_8Si_{13}C_{43}LiO_4H_{117}$	$Sn_9Si_{12}C_{43}LiO_8H_{113}$
formula wt	2043.27	2170.56
T (K)	150	200
cryst syst	monoclinic	orthorhombic
space group	$P2_1/n$	$Fmm2$
a (Å)	16.101(3)	16.765(2)
b (Å)	15.811(3)	24.203(3)
c (Å)	33.193(7)	23.937(2)
α (deg)	90	90
β (deg)	92.69(3)	90
γ (deg)	90	90
V (Å^3)	8441(1)	9712.7(17)
Z	4	4
μ (mm^{-1})	2.613	2.452
δ (g cm^{-3})	1.608	1.484
no. of measd rflns	34 721	50 043
no. of obsd rflns ($I > 2\sigma(I)$)	10 700	4562
R(int)	0.0736	0.0336
GOF	0.998	1.061
Flack param		0.0(2)
R1, wR2 ($I < 2\sigma$)	0.0574, 0.1061	0.0469, 0.1334
R1, wR2 (all data)	0.1030, 0.1184	0.0516, 0.1436

870582 ($\mathbf{6_{Sn}}$) contain supplementary crystallographical data for this paper. These data can be obtained online free of charge at www.ccdc.cam.ac.uk/conts/retrieving.html or from the Cambridge Crystallographic Data Centre, 12 Union Road, Cambridge CB2 1EZ, U.K. (fax, (+44)1223-336-033; e-mail, deposit@ccdc.cam.ac.uk).

■ ASSOCIATED CONTENT

Ⓢ Supporting Information

A table comparing all E−E distances between $\mathbf{6_{Sn}}$ and $\mathbf{6_{Si}}$, a table of the transition energy for the transition from the D_{3h} to the C_{2v} isomer, and CIF files giving crystallographic data for $\mathbf{6_{Si}}$/$\mathbf{6_{Sn}}$ and $\mathbf{6_{Sn}}$. This material is available free of charge via the Internet at http://pubs.acs.org.

■ AUTHOR INFORMATION

Corresponding Author

*Tel: Int. Code +49 (201) 183-3684. Fax: Int. Code +49 (201) 183-2296. E-mail: andreas.schnepf@uni-due.de.

Notes

The authors declare no competing financial interest.

■ ACKNOWLEDGMENTS

We thank the Deutsche Forschungsgemeinschaft (DFG) for financial support and Prof. H. Schnöckel for helpful discussions.

■ DEDICATION

Dedicated to Prof. Günter Schmid on the occasion of his 75th birthday.

■ REFERENCES

(1) Schnepf, A. *Chem. Soc. Rev.* **2007**, *36*, 745−758.

(2) Schrenk, C.; Köppe, R.; Schellenberg, I.; Pöttgen, R.; Schnepf, A. *Z. Anorg. Allg. Chem.* **2009**, *635*, 1541−1548. Pacher, A.; Schrenk, C.; Schnepf, A. *J. Organomet. Chem.* **2010**, *695*, 941−944.

(3) Prabusankar, G.; Kempter, A.; Gemel, C.; Schröter, M.-K.; Fischer, R. A. *Angew. Chem.* **2008**, *120*, 7344−7347; *Angew. Chem., Int. Ed.* **2008**, *47*, 7234−7237.

(4) Brynda, M.; Herber, R.; Hitchcock, P. B.; Lappert, M. F.; Nowik, I.; Power, P. P.; Protchenko, A. V.; Ruzicka, A.; Steiner, J. *Angew. Chem.* **2006**, *118*, 4439−4443; *Angew. Chem., Int. Ed.* **2006**, *45*, 4333−4337.

(5) Desgreniers, S.; Vohra, Y. K.; Ruoff, A. L. *Phys. Rev. B* **1989**, *39*, 10359−10361.

(6) Schrenk, C.; Schellenberg, I.; Pöttgen, R.; Schnepf, A. *Dalton Trans.* **2010**, *39*, 1872−1876.

(7) Schäfer, S.; Assadollahzadeh, B.; Mehring, M.; Schwerdtfeger, P.; Schäfer, R. *J. Phys. Chem. A* **2008**, *112*, 12312−12319. Assadollahzadeh, B.; Schäfer, S.; Schwerdtfeger, P. *J. Comput. Chem.* **2009**, *31*, 929−937.

(8) Oger, E.; Kelting, R.; Weis, P.; Lechtken, A.; Schooss, D.; Crawford, N. R. M.; Ahlrichs, R.; Kappes, M. M. *J. Chem. Phys.* **2009**, *130*, 124305. Lechtken, A.; Debrov, N.; Ahlrichs, R.; Kappes, M. M.; Schooss, D. *J. Chem. Phys.* **2010**, *132*, 211102. Debrov, N.; Oger, E.; Rapps, T.; Kelting, R.; Schooss, D.; Weis, P.; Kappes, M. M.; Ahlrichs, R. *J. Chem. Phys.* **2011**, *133*, 224302.

(9) Scharfe, S.; Fässler, T. F. *Philos. Trans. R. Soc. A* **2010**, *368*, 1265−1284. Sevov, S.; Goicoechea, J. M. *Organometallics* **2006**, *25*, 5678−5692. Fässler, T. F. *Coord. Chem. Rev.* **2001**, *215*, 347−377.

(10) Richardson, A. F.; Eichler, B. E.; Brynda, M.; Olmstead, M. M.; Power, P. P. *Angew. Chem.* **2005**, *117*, 2602−2605; *Angew. Chem., Int. Ed.* **2005**, *44*, 2546−2549.

(11) Schnepf, A. *Angew. Chem.* **2003**, *115*, 2728−2729; *Angew. Chem., Int. Ed.* **2003**, *42*, 2624−2625.

(12) Li, F.; Sevov, S. C. *Inorg. Chem.* **2012**, *51*, 2706−2708.

(13) Schenk, C.; Schnepf, A. *Angew. Chem.* **2007**, *119*, 5408−5410; *Angew. Chem., Int. Ed.* **2007**, *46*, 5314−5316. Schenk, C.; Henke, F.; Santigo, G.; Krossing, I.; Schnepf, A. *Dalton Trans.* **2008**, *33*, 4436−4441. Henke, F.; Schenk, C.; Schnepf, A. *Dalton Trans.* **2009**, *42*, 9141−9145.

(14) Schenk, C.; Schnepf, A. *Chem. Commun.* **2009**, *22*, 3208−3210. Henke, F.; Schenk, C.; Schnepf, A. *Dalton Trans.* **2011**, *40*, 6704−6710.

(15) Fenn, J. B. *Angew. Chem.* **2003**, *115*, 3999−4024; *Angew. Chem., Int. Ed.* **2003**, *42*, 3871−3894.

(16) Gilman, H.; Smith, C. L. *J. Organomet. Chem.* **1967**, *8*, 245−253.

(17) Linti, G.; Köstler, W.; Piotrowski, H.; Rodig, A. *Angew. Chem.* **1998**, *110*, 2331−2333; *Angew. Chem., Int. Ed.* **1998**, *37*, 2209−2211.

(18) Vollet, J.; Stösser, G.; Schnöckel, H. *Inorg. Chim. Acta* **2007**, *360*, 1298−1304.

(19) Schrenk, C.; Kubas, A.; Fink, K.; Schnepf, A. *Angew. Chem.* **2011**, *123*, 7411−7415; *Angew. Chem., Int. Ed.* **2011**, *50*, 7273−7277.

(20) Schnepf, A. *Chem. Commun.* **2007**, 192−194.

(21) Koch, K.; Schnepf, A.; Schnöckel, H. *Z. Anorg. All. Chem.* **2006**, *632*, 1710−1716. Schenk, C.; Henke, F.; Neumaier, M.; Olzmann, M.; Schnöckel, H.; Schnepf, A. *Z. Anorg. Allg. Chem.* **2010**, *636*, 1173−1182.

(22) As all cluster anions $\mathbf{6_{Si}}$, $\mathbf{6_{Si2}}$, and $\mathbf{6_{Sn}}$ appear within the mass range of m/z 1600−1850, mass discrimination due to different ion transfers or detection efficiency is unlikely. In addition, the physical properties of the clusters should be quite similar, as they exhibit the same ligand sphere and the compositions of the cluster cores are quite similar, leading to a resemblance of the intensity of the signals in the gas phase with the concentration in solution.

(23) Quantum-chemical calculations were carried out with the RI-DFT version of the Turbomole program package, by employing the Becke−Perdew 86 functional. The basis sets were of SVP quality. The electronic structure was analyzed with the Ahlrichs-Heinzmann population analysis based on occupation numbers. Turbomole:

Treutler, O.; Ahlrichs, R. *J. Chem. Phys.* **1995**, *102*, 346−354. BP-86 functional: Perdew, J. P. *Phys. Rev. B* **1986**, *33*, 8822−8824. Becke, A. D. *Phys. Rev. A* **1988**, *38*, 3098−3100. RI-DFT: Eichkorn, K.; Treutler, O.; Öhm, H.; Häser, M.; Ahlrichs, R. *Chem. Phys. Lett.* **1995**, *240*, 283−290. SVP: Schäfer, A.; Horn, H.; Ahlrichs, R. *J. Chem. Phys.* **1992**, *97*, 2571−2577. Ahlrichs-Heinzmann population analysis: Davidson, E. R. *J. Chem. Phys.* **1967**, *46*, 3320−3324. Roby, K. R. *Mol. Phys.* **1974**, *27*, 81−104. Heinzmann, R.; Ahlrichs, R. *Theor. Chim. Acta* **1976**, *42*, 33−45. Erhardt, C.; Ahlrichs, R. *Theor. Chim. Acta* **1985**, *68*, 231−245.

(24) A complete list comparing all E−E distances inside the cluster core can be found in the Supporting Information.

(25) Wade, K. *Adv. Inorg. Chem. Radiochem.* **1976**, *18*, 1−66.

(26) In the case of the model compounds with H, Me, Ph, and SiH_3 as ligands, steric influences on the structure by the ligand can be neglected.

(27) A table of the transition energy for the transition from the of the D_{3h} to the C_{2v} isomer for neutral as well as anionic Sn_9R_3 clusters is given in the Supporting Information.

(28) Köppe, R.; Schnepf, A. *Z. Anorg. Allg. Chem.* **2002**, *628*, 2914−2918.

(29) Sheldrick, G. M. *Acta Crystallogr.* **2008**, *A64*, 112−122.